Investigation of breakthrough point variation using a semi-industrial prototype packed with low-cost activated carbon for water purification

Horo Koné[1], Konan Edmond Kouassi[2], Alain Stéphane Assémian[1*], Kopoin Adouby[1], Kouassi Benjamin Yao[1], Patrick Drogui[3]

[1]*Laboratoire des Procédés Industriels, de Synthèse de l'Environnement et des Energies Nouvelles (LAPISEN); Institut National Polytechnique Houphouët-Boigny, BP 1313 Yamoussoukro, Côte d'Ivoire*
[2]*Laboratoire de Thermodynamique et de Physico-Chimie du Milieu (LTPCM), UFR-SFA, Université Nangui-Abrogoua, 02 BP 801 Abidjan 01, Cote d'Ivoire*
[3]*Institut National de la Recherche Scientifique (INRS Eau Terre et Environnement), Université du Québec, 490 rue de la Couronne, Québec City, Canada*

Abstract

The present study was initiated to determine the limit operating conditions of a pre-industrial prototype packed with *Borassus Aethiopum* activated carbon for water purification in rural areas. To do this, the influence of nitrate NO_3^- concentration (38.48; 76.61 mg/L) related to the season (dry or rainy), the flow rate (2; 3 L/min), the mass of activated carbon (260; 300; 380 g) and the height of the filter (15; 20; 25 cm) bed was evaluated. Physico-chemical characterization of the activated carbon prepared has shown a high specific surface (1434.60 m^2/g) with both micro and mesoporous pore structure. For dry season (38.48 mg/L) using Kloze model, the respective breakthrough times of 405.83, 638.38 and 956.67 min were obtained against theoretical times of 420, 630 and 945 min. As for rainy season (76.61 mg/L) predict breakthrough times 332.5, 653.33 and 952 min were found against 315, 525 and 945 obtained theoretically.

1. Introduction

The issue of water resources in general and that of drinking water in particular is a major problem in developing countries, particularly those of sub-Saharan Africa, despite the 97 % of the planet they occupy [1]. This situation is exacerbated by climate change, which contributes to a 53.3 % reduction in river flows [2] and increases turbidity in hot periods by 1.2 to 2.4 NTU [3]. These spatial and temporal variations also have an impact on the variation of nitrates in surface waters, as [4] highlighted in their study on the factors and origins that influence nitrates. Indeed, the presence of nitrate in surface waters has various origins. It has been reported that applied male agricultural practices and wastewater are the main sources [5,6]. In addition, nitrate becomes harmful when it is transformed into nitrite after having been transformed successively into nitrous acid (HNO_2), nitric oxide (N_2O_3), nitrogen dioxide (NO_2), nitrogen monoxide (NO) and then into N-nitrose (RR' NNO) before reaching methaemoglobin (Hb^{3+}) which is harmful to children. Apart from the inconvenience that excess nitrate causes to humans, it is a limiting factor in eutrophication and therefore the cause of the anaerobic state of some stagnant water

bodies such as lakes [7]. One of the difficulties related to this pollutant is its solubility in water which makes its removal difficult [8]. Moreover, the plurality of nitrate-generating sources, especially those related to anthropogenic activities, make this pollutant one of the most abundant in surface waters. This pollution is sometimes such that even the quality of the treated water does not meet safety standards. Several actions are taken to improve this situation. Among these actions, the provision of drinking water supply networks in urban areas. As these drinking water supply systems have very high costs, it would be illusory to think of their generalisation in the context of the current scarcity of financial resources in which developing countries find themselves. As localities with less than 300 souls are left out of the scope of access to drinking water.

It is in this context that a pre-industrial device in an experimental, autonomous and manual phase integrating a local mechanical pump and a filtration system using locally produced activated carbon from *Borassus Aethiopum* has been designed. Testing a device of this size is a first. Indeed, experiments are generally carried out on small prototypes in the laboratory. Adsorption tests are carried out on small columns at the laboratory scale. For instance, [9] used a pilot to remove lead II (Pb^{2+}) on activated carbon. Similarly, fluoride in water on coconut shell-based activated carbon was carried out on a fixed column [10].

Unfortunately, the preparation technique of the activated carbon generally used in these types of laboratory devices is based on the use of modern furnaces (muffle furnace) for the carbonization of biomass. However, in rural areas, such sophisticated devices are most of the time inaccessible and especially increase the final cost of activated carbon production. To get around this constraint, a traditional kiln made from local clay was specially designed. This traditional kiln of very simple design and operation has the advantage of being easily reproducible by the local population. Besides, in order to minimize the cost of manufacturing, branches of *Borassus Aethiopum* (biomass widely available in the area) were used to prepare the activated carbon incorporated inside the prototype filtration columns. The experiments were carried out on a device connected directly to a lake in a real situation.

So, the general objective of this study is to determine the boundary conditions of operation of the prototype designed. Specifically, the influence of parameters such as the height of the size of the filter coal, the initial nitrate concentration and the flow rate are evaluated during the dry and rainy seasons. Finally, the prediction of the breakthrough time of the filters accompanied by a treatment test with several columns will make it possible to limit the risks of contamination and to quantify the treated water.

2. Material and Methods

2.1. Constitutive components of the filtering column

In the first time, the branches of *Borassus Aethiopum* used as precursors are cut and dry for 3 or 4 days at ambient temperature $26 \pm 1\ °C$. Then, artisanal oven was used to carbonize them. During 2 hours, the artisanal oven temperature was maintained at 400 °C by feeding the oven with firewood including a part of *Borassus Aethiopum* branches. After the carbonization, the coal was droughted and sieving using laboratory sieves (3310-1530 Dy 36 LMESHS-Steel /RFS/N 04003699, 0.2 mm x 0.5 mm). The coal was impregnated in a copper sulphate solution ($CuSO_4.5H_2O$) of 1000 ppm for 24 hours before being again heated in a artisanal oven at 550 °C for 2 hours. To finish, 5 hot washes and 5 rinses were necessary and the coal obtained was dried in an oven (MEMMERT) for 24 hours at 105 °C. Just like activated carbon, sand treatment required full steps. To begin, raw sand was taken in the bed of river. Secondly, sand was sieving with laboratory sieves (3310-1530Dy 36 LMESHS-Steel /RFS/N 04003699, 0.2 mm x 0.5 mm) to obtain granular between 0.22 mm and 0.5 mm. Thirdly, the sand was washed and

impregnated in oxygenated water (H_2O_2) at pH= 1.38 for 24 hours to remove organic matter. Then, sand washing was stopped when pH was close to 7. Finally, sand was dried at 105 °C for 24 hours in an oven.

2.2. Characterisation of Borassus Aethiopum activated carbon

2.2.1. Iodine index

This characteristic of activated carbon is representative of its microporosity. In an erlenmeyer flask, 10 mL of 0.2 N iodine solution are introduced and then assayed with a solution of 0.1 N sodium thiosulphate in the presence of a few drops of a starch solution. The dosage ends when all the color has disappeared. Another erlenmeyer flask containing 0.05 g of activated carbon and 15 mL of 0.2 N iodine solution is stirred for 30 minutes. After stirring, a filtration of the new solution is carried out. Then 10 mL of filtrate are removed and then assayed with 0.1 N thiosulfate in the presence of a few drops of a 0.1 N starch solution [11]. The iodine index is calculated by applying the equation (1):

$$Id = \frac{(Vb - Vs).\, N.\, 126,9.\, (\frac{15}{10})}{M} \tag{1}$$

N: normality of the solution of sodium thiosulfate in (mol /L). 126.9: the atomic mass of iodine. M: the mass of the adsorbent in grams.

2.2.2. Methylene blue index

The methylene blue index (mg/g) is an indicator of the capacity of activated carbon to adsorb medium and large organic molecules. This dye is considered to be an indicator of mesoporosity and the study of its adsorption on a porous support reflects the capacity of this material to adsorb the molecules of average molecular weight [12]. The activated carbon was oven dried at 105 °C until the mass stabilized. Firstly, a mass of 300 mg of activated carbon was mixed with 100 mL of 1000 mg/L of methylene blue solution. After stirring for 4 hours, the suspension was filtered and the residual concentration of methylene blue was measured at 650 nm, using UV spectrophotometer (Jasco V530 UV/Vis). Finally, he amounts of methylene blue adsorbed is determined by the following equation (2):

$$IBM = \frac{(C_i - C_f) * V}{m_{CA}} \tag{2}$$

Ci the initial concentration, C_f represent final concentration and m_{CA} indicate the activated carbon mass.

2.2.3. Ash rate

The ash content is a characteristic that makes it possible to judge the carbonization performance. Above 20 %, carbonization is poor and does not favour a better adsorption of pollutants by the activated carbon [11]. His determination was a step-by-step process. Firstly 0.5 g of the dried activated carbon is placed in a dug and placed in an oven (MEMMERT) at 80 °C for 24 hours. After drying the crucible with its contents, it is placed in an artisanal oven set at 650 °C for 3 hours. Once the crucible is removed and cooled to room temperature, the ash content is calculated by considering the equation (3) [20].

$$Ash\ (\%) = \frac{M_3 - M_2}{M_1} \times 100 \tag{3}$$

2.2.4. Moisture

The moisture content is evaluated according to the method used by most researchers such as [11]. Indeed, 0.5 g of activated carbon (M_1) is weighed in a stainless crucible. The crucible and its contents are placed

in an oven at 110 °C to obtain a constant weight of the material before removal (M_3). The material removed from the oven is cooled to room temperature before being weighed (M_2). The rate calculated by equation (4).

$$H(\%) = \frac{M_3 - M_2}{M_1} \times 100 \qquad (4)$$

2.2.5. S_{BET}, pore size, pore volume and diameter evaluation

The Novawin version 11.03 Quantachrome apparatus was used to get the surface BET, the pore volume and the pore diameter. Indeed, a classification of these parameters by UIPAC makes, it possible to judge the activated carbon quality.

2.2.6. Scanning electron microscopy (SEM) analysis

Scanning electron microscopy is a means of assessing the morphology of coal. It was performed using Field Emission Scanning Electron Microscope HITACHI S-4800. To have a good resolution of the image, the activated carbon has been metallized. According to the protocol, 1g of activated carbon is introduced into the device and the reading is done automatically. Several faces of the activated carbon were visualized at different resolution to better appreciate the surface texture and its morphology.

2.2.7. Isoelectric pH of Borassus aethiopum activated carbon

Initial hydrogen potentials (pHi) were obtained by choosing pH values between 2 and 12 which were subsequently adjusted by hydrogen chloride (HCl: 0.1 M) or sodium hydroxide (NaOH: 0.1 M). Following [13] methodology, 50 mL of distilled water, HCl or NaOH solutions were added to obtain the desired pH value. Then, 50 mg activated carbon was added. Hereafter, the mixture was stirred for 24. hours at room temperature (26.4 ± 0.2 °C). Then, the final pH obtained was recorded pH_f. The isoelectric point (zero charge pH) was obtained by plotting the ΔpH curve according to the equation (5) [14]

$$\Delta \quad = \quad - \qquad (5)$$

2.3. Experimental procedure of filtration

The prototype put in place has several elements connected to each other (Figure 1). Lake water (10) was the sample to the prototype test. Indeed, the lake water has fueled the prototype. It is pumped back by a hand pump (1). PVC piping (9) were used again in the place to drive water from the lake to the drilling (7). To finish from the boat to the reservoir for the collection of treated water (6). The circulation of water has been controlled by valves (3). Storage well has been associated to house the discharge pump for raw water to the raw water storage tank. The prototype included activated carbon filters (4) on a 500 L stainless boat that received the treated water (5). The pump was operated by a crank (12) and flow was controlled by a flow meter (8). As for samples, they have been collected periodically after 500 L of treated raw. Also, 100 mL were taken per type of water and then stored for 24 hours at 4 °C in refrigerator before being analyzed. The results obtained were processed with Excel software Microsoft version 2016. Finally, dynamic models such as Dole and Klotz, logistic model and Boltzman were applied to evaluate the effect of several variables (bed height, flow velocity, adsorbent mass and initial concentration). However, the initial and final concentration as well as the pH was determined with spectrometer (Jasco V530 UV/Vis spectrophotometer at 415 nm, Japan) wavelength and pH-meter HANNA (HI991001 Roumanie) respectively. The turbidity was determined using a brand turbidimeter (WTW 430IR Allemagne).

Figure with legend:
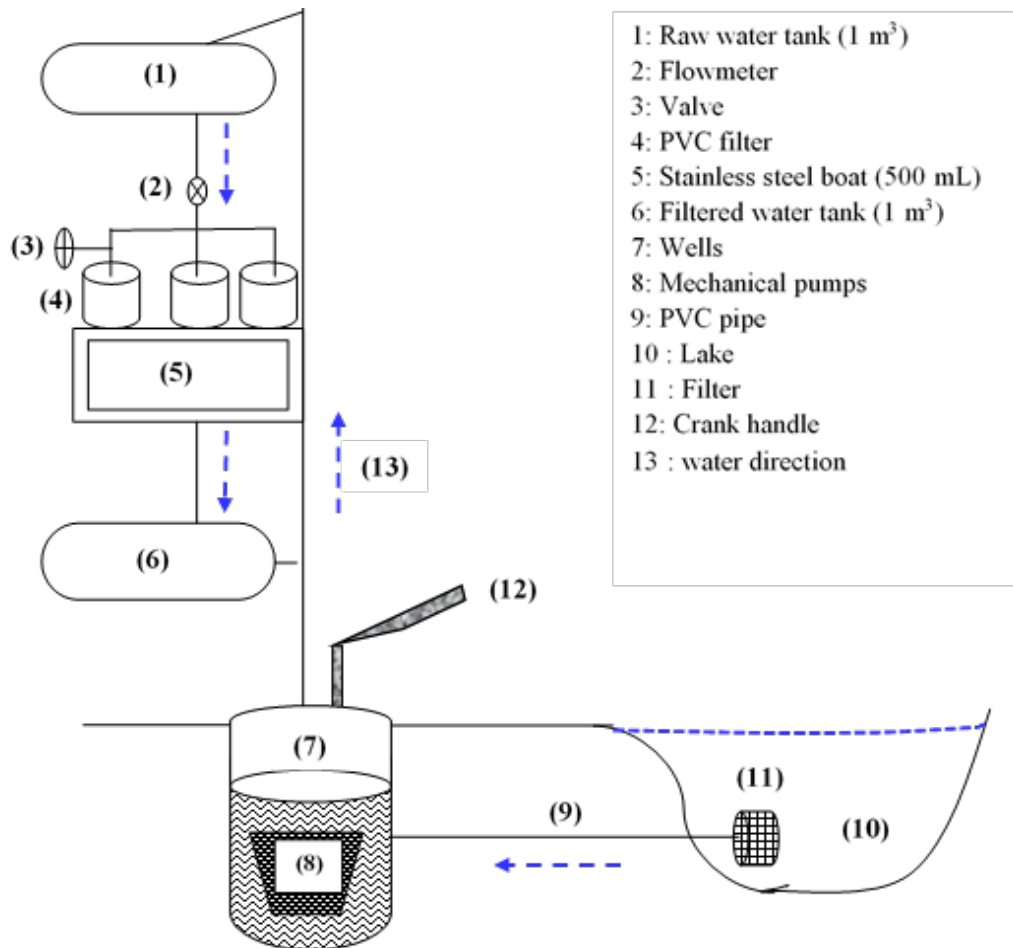
1: Raw water tank (1 m³)
2: Flowmeter
3: Valve
4: PVC filter
5: Stainless steel boat (500 mL)
6: Filtered water tank (1 m³)
7: Wells
8: Mechanical pumps
9: PVC pipe
10 : Lake
11 : Filter
12: Crank handle
13 : water direction

Figure 1: Semi-industrial prototype packed with Borassus Aethiopum activated carbon for water purification

2.4. Dynamic study

2.4.1. Modelling of breakthrough curves by Boltzmann model

Boltzmann model is a model which makes it possible to study the breakthrough curve above all to determine the time t_{50} corresponding to the inflection point. Its initial form is presented by equation (6).

$$A_t = \frac{A_t - A_0}{1 + e^{((t - t_{50/})k}} \tag{6}$$

Considering that at the start of the operation at t=0 the adsorption capacity is zero the initial equation (7) becomes equation (8) :

$$A_t = \frac{A_0 - A_t}{1 + e^{((t - t_{50})/k}} \tag{7}$$

The equation 7 led in this linear form to equation 8 :

$$ln\frac{A_t}{A_0} = \frac{1}{K}(t - t_{50}) \tag{8}$$

2.4.2. Modelling of breakthrough curves by Logistic model

The nonlinear logistic model is a convenient way to model breakthrough curves Eq (9) [15] :

$$A_t = \frac{A_0}{1 + e^{-k(t - t_{50})}} \tag{9}$$

Its simplified form gave the equation (10) :

H. Koné et al., J. Mater. Environ. Sci., 2021, 12(2), pp. 224-243

228

$$ln\left(\frac{A_t}{A_0 - A_t}\right) = k(t - t_{50})\tag{10}$$

In each of these equations, k indicates the rate constant (min^{-1}). At and Ai represents respectively the output concentration and the initial concentration. t and t_{50} represent the time (min) and the time where the initial concentration was eliminated at 50 % respectively. The parameters k and t_{50} were determined by constructing the function $Ln(\frac{A_t}{A_i - A_t}) = f(t)$ where k is the slope of the function and t_{50} is the coefficient [16]. In addition to these two parameters, [16] determined the maximum adsorption capacity, the number of volumes (BV) and the adsorbent exhaustion rate (AER) respectively represented by equations (11)-(12) and (13):

$$N_0 = \frac{A_i}{m}\int_0^{Va}\left(1 - \frac{A_t}{A_0}\right)dv\tag{11}$$

$$BV = \frac{\text{Volume of treated water before breakthrough(L)}}{\text{Volume of adsorbent bed(L)}}\tag{12}$$

$$ARE = \frac{\text{Masse of adsorbent (g)}}{\text{Volume of water treated before the breakthrougg point(L)}}\tag{13}$$

The breakthrough curves of the logistic regression model were represented by the function $\frac{A_t}{A_0} = f(t)$. When A_t constituted the concentration out of the filter, A_0 the initial concentration and v_t the volume at the instant t.

2. 4.3. Prediction of breakthrough time
The bed service time theory was initiated by Dole and Klotz (1946). They make simply combining the Adams and Bohart model with that of Thomas to give the equation (14):

$$Ln\left(\frac{A_0}{A_t} - 1\right) = Ln\left(e^{kq_0\frac{H}{U}} - 1\right) - kA_0 t\tag{14}$$

Starting from this relation, the time t was determined according to the equation (15):

$$t = \frac{N_0}{A_i u} * H - \frac{1}{kA_0}Ln\left(\frac{A_0}{A_t} - 1\right)\tag{15}$$

The prediction time and the breakthrough front were determined from equation (16):

$$t_a = \frac{N_0}{UA_0}(H_i - H_0)\tag{16}$$

Indeed, the representation of $t_a = f(H)$ allowed to calculate the adsorption capacity and predict time.

2.4.4. Error calculation
During regression nonlinear study, [17] used least square of errors method in non-linear regression analysis. The errors were calculated according to the equation (17) [18]. The model with the lowest values is the one that will better describe the *Borassus Aethiopum* activated carbon breakthrough curves. Calculations were performed with Excel 2016 software as well as all breakthrough curves:

$$SS = \frac{\sum_0^n\left[(\frac{A_t}{A_i})_{cal} - (\frac{A_t}{A_i})_{exp}\right]}{N}\tag{17}$$

3. Results and discussion

3.1. Characteristic of Borassus Aethiopum activated carbon

After activation, the iodine number and the methylene blue index are 958.09 mg/g and from 28.8 mg/g, respectively (Table 1). In fact, the higher iodine number and the methylene blue index, showed that coal is better quality. As for the rate of 2.89 % ash obtained, it can say that the activated carbon, got the conditions of a good adsorbent according to [19] who affirmed that ash rate must not exceed 6 %. This ash rate is also comparable to that of other researchers such as [20] who obtained values varying from 3 to 12 % for different activated carbon obtained with *rachis Hypogea* and *Vigna Radiata*. Thus, the *Borassus Aethiopum* activated carbon prepared in a traditional oven underwent good carbonization. Indeed, 2.89 % is much lower than 20 % which is the value beyond which carbonization is considered insufficient [20].

Table 1: Characteristics of *Borassus Aethiopum* activated carbon prepared by artisanal method

Parameters	Values	Unit
Iodine index	958.09	mg
Methylene Blue index	28.8	mg/g
Ash rate	2.89	%
pH	5	-
BET surface (S_{BET})	1431.61	m^2/g
Micropor surface (S_{mic})	1074	m^2/g
S_{ext} / S_{BET}	75	%
External surface (S_{ext})	1432	m^2/g
Total pore volume (V_{pt})	0.97	cm^3/g
Micropor volume (Vmicr)	0.279	cm^3/g
C	4.929	-
Pore diameter (DFT)	2.76	nm
Pore diameter (BJH)	1.853	nm
Pore diameter (DH)	1.853	nm
Pore diameter (HK)	1.847	nm

Based on the iodine number, the methylene blue index and the ash content, it can be stated that the *Borassus Aethiopum* carbon prepared under less severe conditions remains competitive and a good adsorbent. In addition, this activated carbon is able to adsorb small molecules as well as large molecules. Thus, the activated carbon has an acidic character while the one that is not activated is rather basic with a pH of 8.02. Ortho phosphates were evaluated because of the richness of the phosphorus *Borassus Aethiopum* plant [21]. Since the maximum rate of ortho phosphate was set at 0.4 mg/L by WHO, (2011). With regard to the specific surface obtained by the BET theory carried out using the cantachrom apparatus, it can be affirmed that the *Borassus Aethiopum* activated carbon is a competitive carbon. Indeed, the specific surface obtained belongs to the interval [500; 1500] m^2/g defined by IUPAC for commercial activated carbon.

3.2. Pore size distribution

The pore distribution was determined by DFT method. Figure 2 shows the evolution of pore volume as a function of pore size. It shows a relatively constant evolution of the pore volume from 2.3129 with a peak at 2.6472 nm corresponding to a volume of 0.6298 $cm^3.nm^{-1}.g^{-1}$. Pore diameters between 2 and 50 nm indicates a mesoporous structure for the activated carbon according to IUPAC classification.

However, the different diameters obtained by different methods using Quantachrome Novawin 11.03 reveals the presence of micropores. Indeed, the model Barrett, Joyner, Halenda (BJH) and Horvath-Kawazoé (HK) methods provided respective diameters 1.853 and 1.847 nm which are all < 2 nm So, *BorassusAaethiopum* activated carbon should probably contain micropores in addition to mesopores as shown by the high iodine value obtained (table 1).
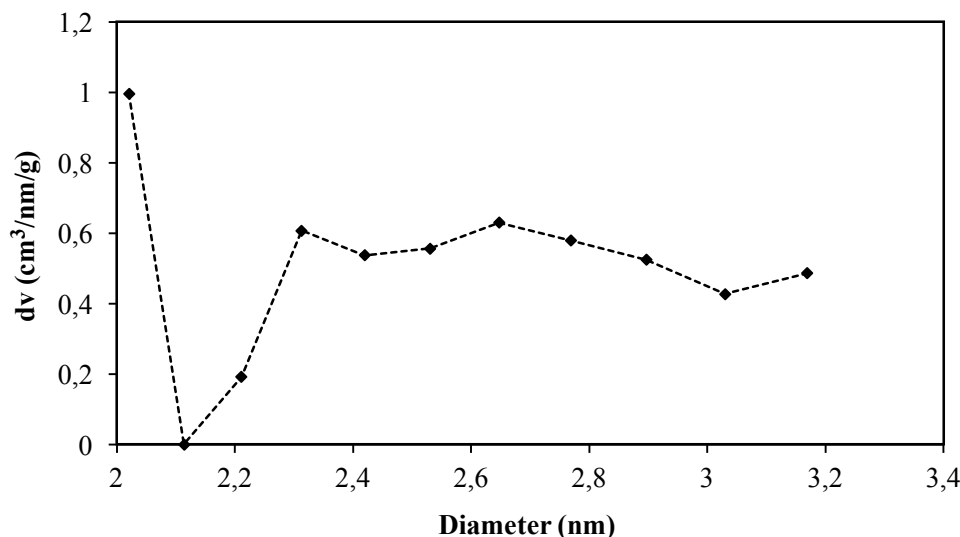
Figure 2: Pore distribution obtained using DFT model

3.3. *Borassus Aethiopum* carbon morphology

Scanning electron microscope analysis allowed to visualize activated carbon surface morphology and allowed to better appreciation the pore size distribution (Figure 3). Then, the photograph showed that activated carbon from *Borassus* fibers contained several types of pores. Indeed, we can clearly observe that these pores have elongated and spherical shapes distributed in a heterogeneous way.
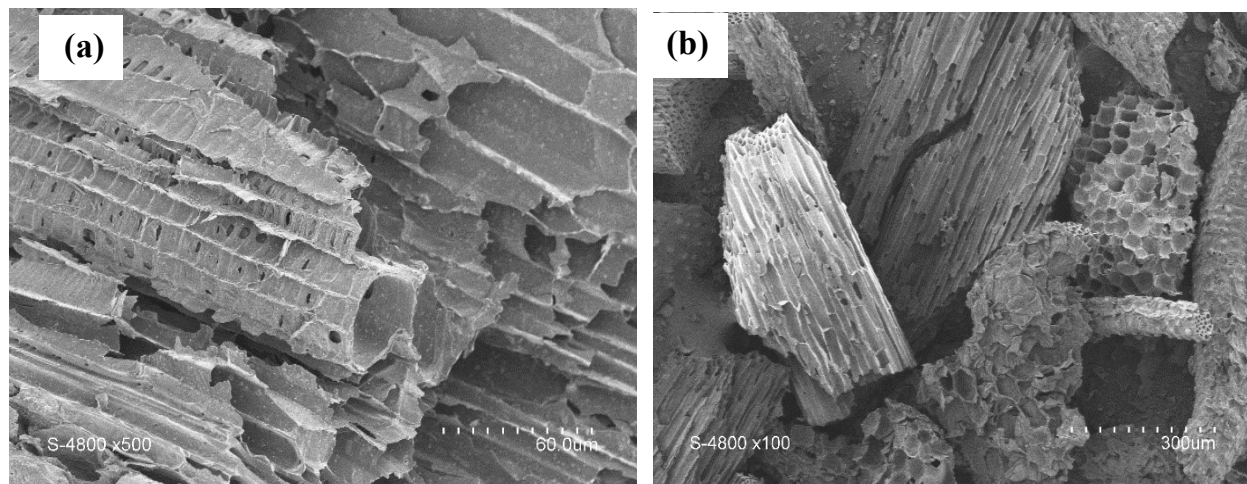
Figure 3: Morphological analysis of Borassus Aethiopum activated carbon

3.4. *Initial raw water characterization*

Nitrate and pH were evaluated on the raw water of lake (Table 2). Mean values of 76.61 ± 0.8 mg/L and 6.73 ± 0.2 were observed during the rainy period, compared to 38.48 ± 0.2 mg/L and 6.41 ± 0.1 during drought periods. The seasonal variation of nitrate concentrations was very highly significant (p-value = 7.10^{-7}). In fact, the runoff water fed the lake, and provided nitrate enriched residues from the

surrounding fields. This finding was also made by [1] who obtained an increase of 5.12 ± 0.44 in the rainy season. The pH with a less significant difference (p-value = 0.04584 > 0.005) decreased slightly in the dry season. This decline in the dry season was related to a transformation of organic matter into humic acid according to [1]. Indeed, they found average values of 6.8 in the dry season against 7 in the Rainy season. In addition to the nitrate ions and the Ph, other physicochemical parameters were evaluated even if this study does not specifically focus on them (Table 2)

Table 2: Physico-chemical characteristics of raw water according to dry and rainy seasons

Parameters	Unit	Dry season	Rainy season	(WHO, 2011)
Temperature	°C	28.2 ± 1	26.85 ± 1	< 30
pH	-	6.41 ± 0.1	6.73 ± 0.2	6.5-8.5
Turbidity	NTU	7.83 ± 0.4	5.75 ± 0.2	< 1
Mg^{2+}	mg/L	0.162 ± 0.02	0.164 ± 0.03	-
Hardness	mg/L	0.333 ± 0.01	0.315 ± 0.02	≤ 30
Ca^{2+}	mg/L	6.06 ± 0.03	6.295 ± 0.025	-
PO_4^{3-}	mg/L	0.01 ± 0.001	0.02 ± 0.001	< 0.4
$CaCo_3$	mg/L	0.583 ± 0.015	0.726 ± 0.01	-
Conductivity	µS/cm	154.95 ± 1.6	254.45 ± 1.4	200-1000
NO_3^-	mg/L	38.48 ± 0.45	76.61 ± 1.05	< 50
COD	mg/L	82.18 ± 0.190	58.88 ± 1.3	< 30

3.5. Influence of pH on nitrate removal

The pH of the raw water was evaluated because it affects the pH of the activated carbon zero charge. Indeed, the pH of zero charges was 5 and the average pH of the lake water is 6.41 ± 0.1 in the dry season and 6.73 ± 0.2 in the rainy season. Then, the adsorption of the nitrate ion (NO_3) was negatively influenced because the pH= 6.41 ± 0.1 and 6.73 ± 0.2 higher than pH= 5 created an increasing of negative charge on activated carbon [22]. This negative polarity change of the activated carbon makes it more attractive to cations [22].

3.6. Influence of column height on the breakthrough time

The construction of $A_t/A_0 = f (t)$ columns at different heights allowed to study the bed height influence. The flow rate (q) of the water in the columns was fixed at 2 L/min. This influence study of the bed height on the breakthrough point gave the Figures (4a and 4b). The breakthrough times of 420 min, 630 min and 735 min were determined corresponding to A_t/A_i=0.331, A_t/A_i=0.214 and A_t/A_i=0.101 respectively for 15 cm, 20 cm and 25 cm when initial concentration is 38.48 mg/L (dry season; Figure 4a). As for the rainy season (Ai=76.61 mg/L; Figure 4b), breakthrough time 315 min, 420 min and 525 min were obtained for heights of 15, 20 and 25 cm corresponding to A_t/A_i=0.15, A_t/A_i=0.12 and A_t/A_i=0.1 respectively. We remark that the breakthrough time increase with bed increasing. Indeed, an increase in the column height leads to an increase in the contact time and the active sites. The adsorption time being long. His positively influences the breakthrough time which becomes long to nitrate contact time and active sites being important. The adsorption time is important. The same observation was made by [23]. Indeed, they found breakthrough time 1121.38; 1987.71 and 6395.33 min respectively for bed height 2, 4 and 8 cm.
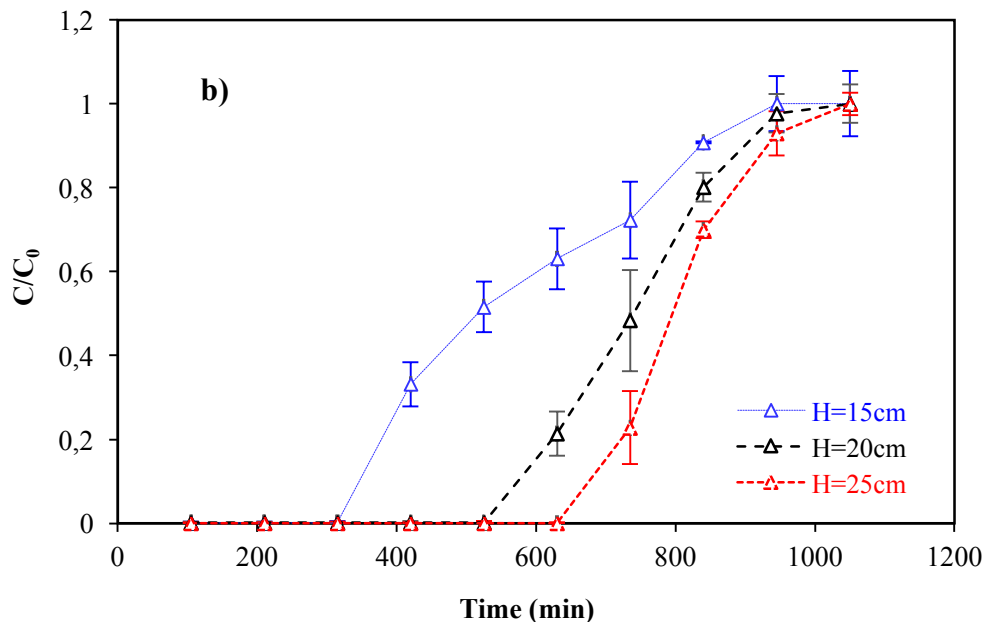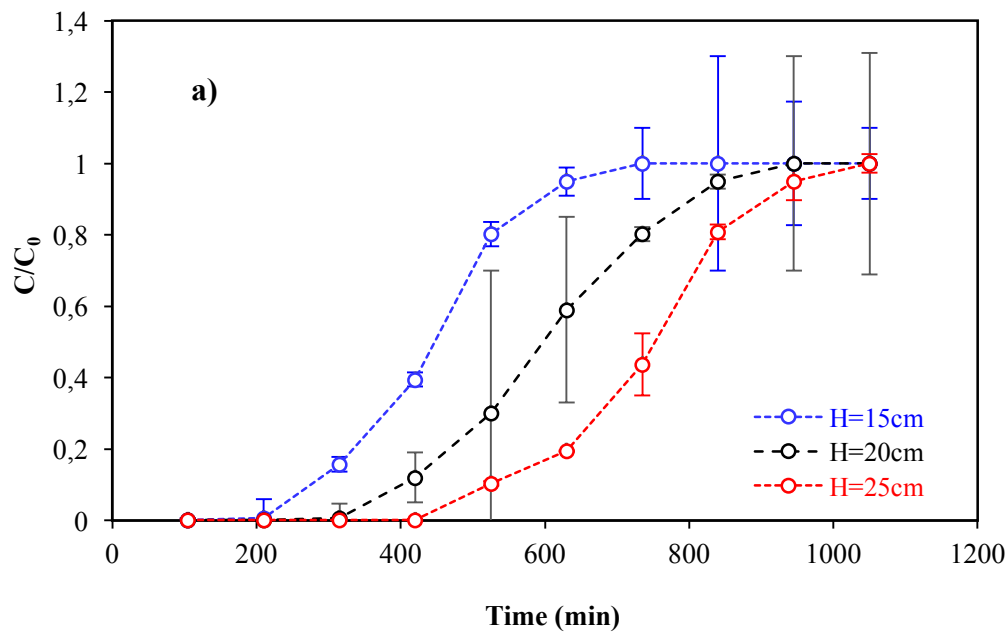
Figure 4 : Nitrate breakthrough curves for three height filters (15 cm, 20 cm and 25 cm) as a function of dry season ((4a): 38.48 mg/L) and rainy season ((4b): 76.61 mg/L)

3.7. Influence of raw water quality on the breakthrough time

Initial concentration influence was study by three bed height (15 cm, 20 cm and 25 cm) considering initial concentrations of nitrate 38.48 mg/L and 76.61 mg/L as seen in figure 5. Based on these breakthrough curves, it can say that for identical bed heights, the breakthrough time was influenced by the nitrate concentration that passed through the filter bed. Indeed, for beds height (15 cm, 20 cm and 25 cm), breakthrough time were 315 min and 420 min for bed height 15 cm (Figure 5a) corresponding to $A_t/A_i = 0.157$ and $A_t/A_i = 0.331$. For bed height 20 cm (Figure 5b), 420 min and 630 min were got to $A_t/A_i = 0.12$ and 0.214 respectively. To finish, considering 25 cm of bed height (Figure 5c), breakthrough time 525 min at $A_t/A_i = 0.103$ and 735 min at $A_t/A_i = 0.22$ for 25 cm.
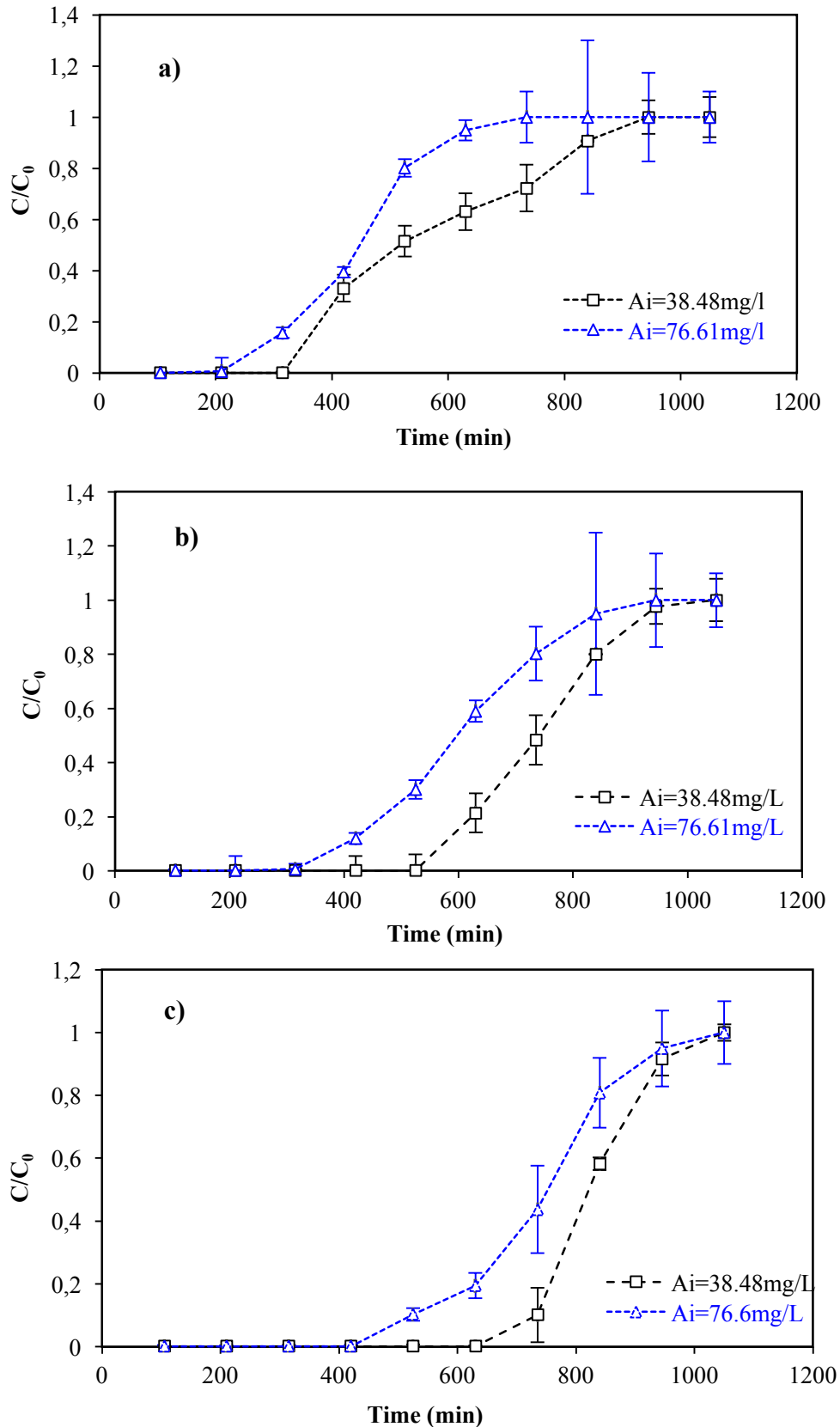
Figure 5: Nitrate breakthrough curves as a function of dry (38.48 mg/L) and rainy season (76.61 mg/L) for three beds height ((a): 15 cm; (b): 20 cm and (c): 25 cm)

We can remark that the breakthrough time decrease with the increase of nitrate concentration. In other words, the breakthrough time is reducing when moving from dry (38.48 mg/L) to rainy season (76.61

mg/L) where the nitrate content in the lake is almost double. This reduction in the breakthrough time in the rainy period with a concentration of 76.61 mg/L is linked to a reduction in the so-called active agent of the activated carbon. In fact, the higher the concentration, the higher the number of molecules adsorbed. Thus, several active carbon sites are occupied in a reduced time, hence the smallest breakthrough times observed for the concentrations of 76.61 mg/L regardless of the column considered. Similarly, observation was made by [23]. Indeed, they got values 6395 min and 3281 min breakthrough time respectively for 30 and 40 mg/L initial concentration when bed height was 4 cm. Also, Onyango et al. [16] made the same observation. They found the breakthrough time 1211 and 573 min respectively for 5 and 10 mg/L as initial concentration. For the same initial concentrations of the rates of 1.33 and 0.8 were obtained. Similarly, observations were made by [24]. They found breakthrough times of 60 and 18 min respectively at concentrations of 20 and 30 mg/L.

3.8. Influence of flow rate on the breakthrough time

Figure 6 show the flow rate influence on breakthrough time. The analysis of the results show that the breakthrough time decreases when flow rate increases from to 2 L/min to 3 L/min. Considering 15 cm as bed height and flow rate (2 L/min and 3 L/min), we obtained 315 min and 420 min corresponding to At/Ai=0.0736 and At/Ai=0.0528 respectively (figure 6a). As for bed height 20 cm (figure 6b), with flow 2L/min and 3L/min, 420 min and 525 min breakthrough time were got corresponding to At/Ai= 0.0966 and 0.0759 respectively. Concerning bed height 25 cm (Fig. 6c), breakthrough time were 525 min at At/Ai= 0.0966 and 735 min at At/Ai = 0.14. Furthermore, the increase in flow rate implies an increase in the filtration rate. However, the higher the filtration speed, the less the contact time. More explicitly, this lack of contact limits the efficiency of nitrate ions to be adsorb onto activated carbon surface et consequently causes it presence in the filtrate. In addition, the increase in the flow rate in the columns could also lead to an increase in the rate of desorption of pollutants by a leaching phenomenon. Hence, the early breakthrough for the flow rate of 3L/min compared to 2L/min. The same observation was made by [15] , [25] and [23] . Indeed, [15] found 3600 min and 2040 min respectively for 2 mL/min and 5 mL/min as flow rate. In the same way, [23] found 4813.04 min and 2102 min respectively for 0.5 mL/L and 2 mL/L. As for [25] breakthrough times of 10 and 1 hours were obtained for respective flow rates of 1.5 and 2.9 mL/min. The short breakthrough times obtained with the flow rate of 3L/min are certainly due to a lack of intimate contact between the raw water and the coal column. Indeed, the further the flow rate deviates from 0.3 m/s as predicted by [26] and [27] the less efficient the treatment.

3.9. Comparison of Logistic and Boltzmann models

Bed height, flow velocity, adsorbent mass and initial concentration were the parameters used to evaluate the two models. The values are summary in table 3. With this model, the time t_{50} and k were evaluated. Considering one of these models it appeared that the breakthrough time t_{50} increase with the adsorbent mass and adsorbent height but, it decreases with flow rate and initial concentration increase. When bed height varying 15 cm to 25 cm, breakthrough time t_{50} were increased of 758.87 to 973.094 min for Logistic model against 856.253 to 1038.16 min for Boltzman model. This observation is in agreement with that of [26] who found 17 and 22 min for the respective columns of 15 and 22 cm. However, this time decrease of 962.155 to 859.25 min when the initial concentration increases to 38.48 mg/L to 76.61 mg/L. In the same way, the breakthrough time t_{50} decrease of 833.477 to 762.787 when flow rate increase of 2 mL/L to 3 ml/L considering Logistic model and 962.422 to 863.577 with Boltzman model. This variation was made by [15] during his study on breakthrough analysis of continuous fixed-bed adsorption of sevoflurane using activated carbon. Along with the removal of nitrate from the lake water, turbidity

was eliminated. It emerges from the table analysis that the breakthrough times considering to the logistic model and the Boltzmann model are approximately identical.
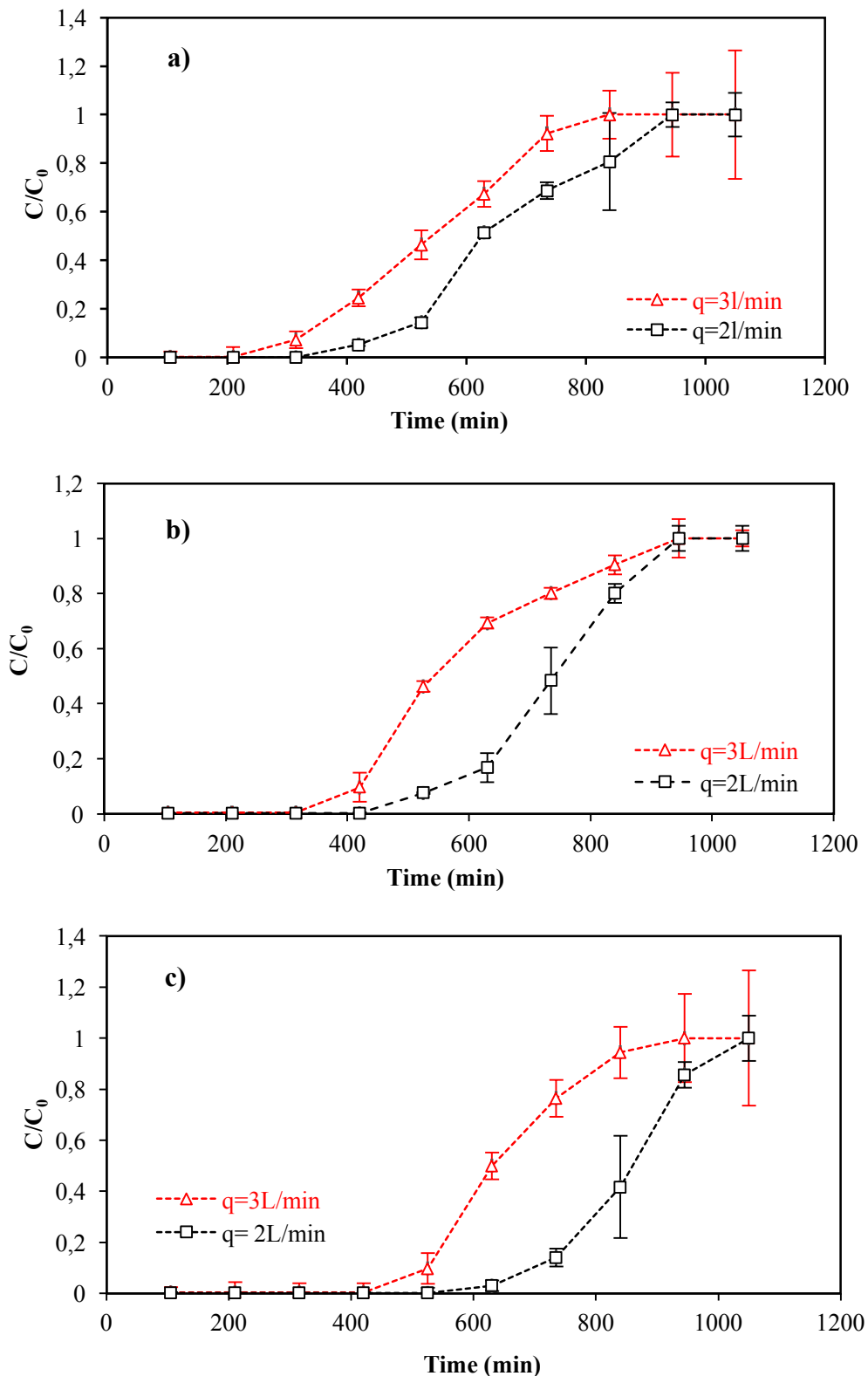
Figure 6: Nitrate breakthrough time variation as a function of flow rate (2 L/min; 3L/min) under dry season (38.48 mg/L) for three beds height ((a): 15 cm; (b): 20 cm and (c): 25 cm)

Indeed, for a height of 15 cm of bed, the breakthrough times are 794.526 and 758.875 min then 841.417 and 856.253 min respectively for logistic model and Boltzmann model for the adsorption of nitrate and turbidity removal. When at the bed height column 20 cm, the breakthrough times are 833.923 and

833.477 min for the logistic model then 891.5 and 962.422 min for the Boltzmann model. Finally, for 25 cm, breakthrough times 915.461 and 973.094min were obtained for the logistic model respectively for turbidity and nitrate then from 967.769 and 1038.16 min for Boltzmann model.

Table 3: Summary of model parameters for water treatment using Borassus Aethiopum activated carbon

Parameters	Logistic model				Boltzmann model			
	t_{50} (min)	K (min^{-1})	R^2	RMSD	t_{50} (min)	K (min^{-1})	R^2	RMSD
	Bed height (C_0=38.48 mg/g)				Bed height (C_0=38.48 mg/g)			
15 cm	758.87	0.009	0.67	0.31	856.25	126.58	0.73	1.215
20 cm	833.48	0.011	0.78	0.35	962.42	111.11	0.82	0.427
25 cm	973.09	0.009	0.73	0.24	1038.16	80	0.77	0.217
	Flow Velocity (C_0=38.48 mg/g)				Flow Velocity (C_0=38.48 mg/g)			
2 L/min (15cm)	758.87	0.008	0.67	0.31	856.25	126.58	0.73	1.215
3 L/min (15cm)	758.71	0.006	0.62	0.34	847.46	163.93	0.77	0.254
2L/min (20cm)	833.48	0.011	0.78	0.35	962.42	111.11	0.82	0.427
3L/min(20cm)	762.79	0.008	0.71	0.34	863.58	140.84	0.80	0.149
2L/min (25cm)	973.09	0.009	0.73	0.24	1038.16	80.00	0.77	0.217
3L/min (25cm)	810.62	0.008	0.74	0.63	909.89	129.87	0.84	0.223
	Adsorbent mass (C_0=38.48 mg/g)				Adsorbent mass (C_0=38.48 mg/g)			
260 g	758.87	0.008	0.67	0.31	856.25	126.58	0.73	1.215
300 g	833.48	0.011	0.78	0.35	962.42	111.11	0.82	0.427
380 g	973.09	0.009	0.73	0.24	1038.16	80.00	0.77	0.217
				Initial concentration	Initial concentration			
76.61 mg/L (15cm)	812.31	0.006	0.46	0.31	679.88	163.93	0.60	4.233
38.48 mg/L (15cm)	758.87	0.008	0.67	0.31	856.25	126.58	0.81	1.215
76.61 mg/L (20cm)	859.92	0.008	0.76	0.72	762.82	109.89	0.83	3.045
38.48 mg/L (20cm)	962.15	0.009	0.82	0.35	962.42	111.11	0.82	0.427
76.61 mg/L (25cm)	932.47	0.009	0.86	0.53	922.34	109.89	0.88	0.714
38.48 mg/L (25cm)	973.09	0.009	0.73	0.24	1038.16	80.00	0.77	0.217

3.10. Competitive effect of turbidity

Turbidity is one of the first physicochemical parameter to be checked when filtering water on a column. It can directly alter the performance of a filtration column due to the affinity of colloidal particles for porous materials such as activated carbons. Hence, table 4 shows the evolution of breakthrough points for turbidity and nitrate removal as a function of a bed's height and the season. Results obtained show us that during the dry season (38.48 mg/L) for a bed height of 15 cm for instance, the breakthrough time for turbidity corresponds to 650.7 min while it reaches 758.87 min for nitrate. Breakthrough points studied over two periods of the year (dry and rainy) showed that turbidity is the limiting factor overall. Indeed, the smallest filter breakthrough times for turbidity are obtained regardless of the Logistic or Boltzman model. Since turbidity is caused in part by the colloidal particles, it can therefore limit the adsorption of nitrates on activated carbon surface by competition phenomenon. Let us notice that

colloids particles are either electronegative (like nitrate) and hydrophilic (clays, humus for example, with the presence of amine or alcohol groups can create an H bond with water), or electropositive and hydrophobic (minerals such as iron oxides, alumina oxides, and starch). As the pH of the lake water is between 6 and 7, the surface of the carbon will be negatively charged. Colloids are negatively charged in water. Thereby, they cause an electrostatic repulsion which will prevent their adsorption, thus reducing the breakthrough time. On the other hand, according to [22], nitrate ions adsorption is better at pH 7. Therefore, with regard to the pH of the raw water, in accordance with [22], the adsorption of nitrate ions is favourable, hence a significant breakthrough time.

Table 4: Comparisons of turbidity and nitrate breakthrough times variation

Parameters	Logistic model				Boltzmann model			
	t_{50} (min)	K (min^{-1})	R^2	RMSD	t_{50} (min)	K (min^{-1})	R^2	RMSD
7.83 NTU (15cm)	650.70	0.005	0.69	0.06	794.53	109.89	0.76	0.175
38.48 mg/L (15cm)	758.87	0.008	0.67	0.31	856.25	126.58	0.73	0.121
7.83 NTU (20cm)	776.65	0.009	0.84	0.09	833.92	83.33	0.89	0.154
38.48 mg/L (20cm)	833.48	0.011	0.78	0.35	962.42	111.11	0.82	0.427
7.83 NTU (25cm)	800.65	0.014	0.93	0.77	915.46	76.92	0.95	0.097
38.48 mg/L (25cm)	973.09	0.009	0.73	0.24	1038.16	80.00	0.77	0.217
5.75 NTU (15cm)	794.53	0.009	0.70	0.61	841.00	109.89	0.76	0.18
76.61 mg/L (15cm)	812.31	0.006	0.50	0.31	679.88	163.93	0.60	4.233
5.75 NTU (20cm)	833.92	0.013	0.84	0.55	891.5	83.33	0.89	0.126
76.61 mg/L (20cm)	859.92	0.008	0.76	0.72	762.2	109.89	0.83	3.045
5.75 NTU (25cm)	915.46	0.014	0.93	0.14	967.77	76.92	0.95	0.07
76.61 mg/L (25cm)	932.47	0.009	0.86	0.53	922.34	109.89	0.88	0.714

3.11. Bed volumes (BV) and adsorbent exhaustion rate (AER)

The influence study of bed volumes (BV) and adsorbent exhaustion rate (AER) made it possible to obtain the parameters summarized in Table 5. Considering the same masses of activated carbon 260 g for the first series, 300 g for the second and 380 g for the third series for concentrations of 38.48 mg/L and 76.61 mg/L BV increased and AER decreased. We obtained 382.16; 398.09 and 424.63 for BV against 0.13; 0.12 and 0.11 g/L for AER respectively for 260 g, 300 g and 380 g with 38.48 mg/L as initial concentration. Considering [15] assertion who consider the lowest values of AER as an indicator of good column performance, we can say that the column with a bed mass of 380 was the best performer. Indeed, an AER value of 0.108 g/L was obtained for 380 g against 0.13 and 0.12 respectively for 260 g and 300 g of bed mass. The analysis of the table also shows that the AER are influenced by the initial concentration which passes through the filter. Indeed, for three columns of mass 260 g, 300 g and 380 g and initial concentrations of 38.48 and 76.61 mg/L, the AER and BV were respectively 0.13; 0.17 and 212.31; 382.16 for 260 g. When in the mass was 300 g column, values of 0.12; 0.15 and 398.09; 238.86 and finally for 380 g values of 0.11, 0.12 and 423.63; 318.47min were obtained. It appears that the AER increase with concentration while the BV decreases. This remark is in agreement with that of [16] do. Indeed, they found AERs of 1; 2.1 and 3.8 and BV 1177; 557 and 300 respectively for concentrations 5.10 and 20 mg/L in his study on breakthrough analysis for water defluorination using surface-tailored

zeolite in a fixed bed column. Also, [15] found through their study on fixed bed water disinfection which gave BV 283 and 216 then AER 1.6 and 2.1 g/L for concentrations of 660 CUF/mL and 6000 CUF/mL. In addition to the influence of parameters such as mass, concentration, influence of flow rate was evaluated. Thus, we can deduct from the analysis of the table that the flow rate increase leads to an increase in the values of AER. Hence, the decrease of the filter columns performance is in accordance with [15] results.

Table 5: Summary of results at breakthrough point as a function of different parameters

Parameters	Service time	AER (g/L)	BV	N_0 (mg/g)
Bed heigh				
15 cm	420	0.13	382.17	253.08
20 cm	630	0.12	398.09	301.55
25 cm	945	0.11	424.63	304.66
Flow Velocity				
2 L/min (15 cm)	420	0.13	382.16	253.08
3 L/min (15 cm)	315	0.17	106.16	267.39
2 L/min (20 cm)	630	0.12	398.09	301.55
3 L/min (20 cm)	420	0.15	159.24	289.67
2 L/min (25 cm)	945	0.11	424.63	304.66
3 L/min (25 cm)	525	0.13	191.08	304.66
Adsorbent mass				
260 g	420	0.13	382.16	253.08
300 g	630	0.12	398.09	301.55
380 g	945	0.11	424.63	304.66
Initial concentration				
76.61 mg/L (15 cm)	210	0.17	212.31	369.93
38.48 mg/L (15 cm)	420	0.13	382.16	369.93
76.61 mg/L (20 cm)	420	0.15	238.85	457.59
38.48 mg/L (20 cm)	630	0.12	398.09	301.55
76.61 mg/L (25 cm)	525	0.13	318.47	516.01
38.48 mg/L (25 cm)	945	0.11	424.628	304.66

3.12. BDST application

Dole and Klotz (1946) model allowed to evaluate the filter service times (BTSD) and adsorption capacities summarize in Table 6. The prediction times were obtained through the equations following the construction of the breakthrough time data corresponding to the ratios At/Ai = 20 %, At/Ai = 70 % and At/Ai = 90 % of each column. Prediction times of 405.83, 638.33 and 956.67 min correspond to drying season (38.48 mg/L) whereas prediction time of 332.5, 653.333 and 952 are for the rainy season (76.61 mg/L). The correlation coefficients 0.95, 0.9876 and 0.993 obtained during dry season (Figure 7a) and 0.949, 0.983 and 0.964 in rainy season made it possible to say that the BDST well described the columns (Figure 7b). By comparing the experimental breakthrough times of 420, 630 and 945 to the respective prediction times 405.83; 638.33 and 956.67 min in drying season (38.48 mg/L) and experimental breakthrough time of 315; 525 and 945 min to respective prediction time 332.5; 653.333 and 952 during the rainy season (76.61 mg/L), we can conclude that the models selected to describe the prototype are reliable. These results are comparable to those obtained by [27]. Indeed, the authors obtained an experimental breakthrough time of 480 min against a prediction time of 503.65 min.

Table 6: Comparison between experimental service time and predicted service time

Season	Ai (mg/l)	Height (cm)	A_t/A_0	N_0' (mg/l)	K_D' (L.mg^{-1}min^{-1})	Breakthrough time (min)	Predict time (min)
	38.48	15	0.51	343.13	1.1090×10^{-4}	420	405.83
	38.48	20	0.48	257.35	9.7441×10^{-5}	630	638.33
Dry	38.48	25	0.58	205.88	1.5732×10^{-4}	945	956.67
	76.61	15	0.39	388.29	8.940×10^{-5}	315	332.5
	76.61	20	0.59	364.45	1.060×10^{-4}	525	653.33
Rainy	76.61	25	0.43	270.81	1.154×10^{-4}	945	952
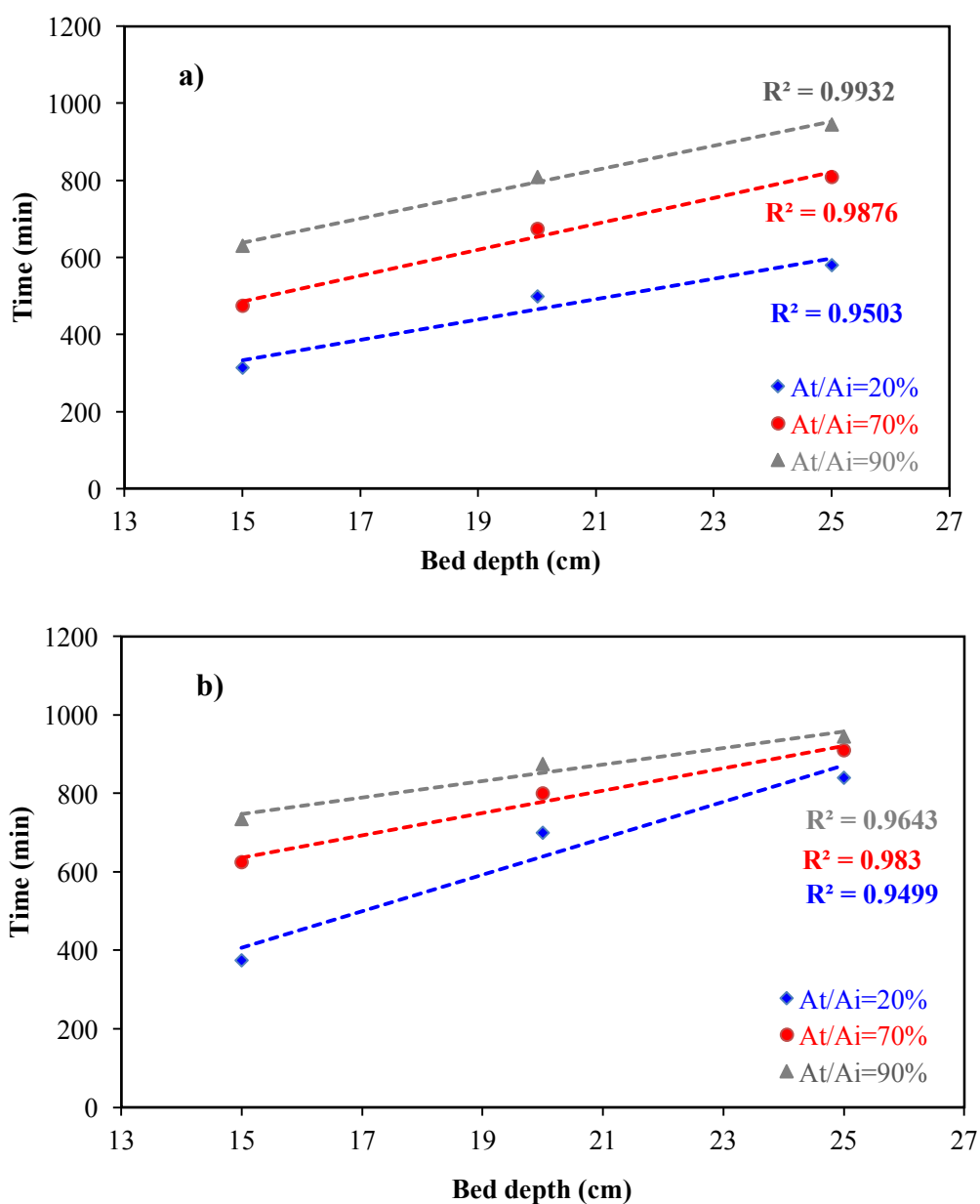
Figure 7: Bed depth versus service time plot at different values of At/Ai in fixed-bed column for the nitrate removal in dry ((a): Ai=38.48 mg/L) and rainy season ((b): Ai=76,61 mg/L)

Conclusion

In view of the characteristics of *Borassus Aethiopum* activated carbon, it can be said that it is a good adsorbent, especially with its high specific surface of 1431.32 m^2/g. Also, the precursor used is suitable for the production of activated carbon because ash rate is less than 20 %. In addition, *Borassus Aethiopum* activated carbon contains mesopores of irregular sizes and micropores following pore size distribution and scanning electron microscopic analysis. Studying the breakthrough curves of *Borassus Aethiopum* activated carbon has made it possible to determine the life of coal in rainy and dry periods. For three columns of heights 15; 20 and 25 cm breakthrough time were respectively 315; 525 and 945 min to min for the rainy season (76.61 mg/L) and 420, 630 and 945 for the dry season (38.48 mg/L). It has also been shown that the concentration of the pollutant, the column height, the flow rate and wear of the adsorbent influence the life of the filter. The prediction model perfectly describes the adsorption of nitrate because the predicted values (405.83; 638.33 and 956.67 min) which are close to the experimental ones (420, 630 and 945 min). Finally, this study proves that this semi-industrial prototype designed for water purification can be used a community scale. So, its popularization can therefore be seriously considered.

References

[1]   A. Pratap, P. Bisen, B. Loitongbam, P. Singh, "Assessment of Genetic Variability for Yield and Yield Components in Rice (Oryza sativa L.) Germplasms", *International Journal of Bio-Resource and Stress Management*. 9 (2018) 87–92. https://DOI:10.12691/ajwr-6-4-1

[2]   T. Gadissa, M. Nyadawa, F. Behulu, B. Mutua, "Assessment of catchment water resources availability under projected climate change scenarios and increased demand in Central Rift Valley Basin, in: Extreme Hydrology and Climate Variability", *Elsevier*, (2019) pp. 151–163. https://DOI:10.12691/ajwr-7-1-4

[3]   H. Mi, S. Fagherazzi, G. Qiao, Y. Hong, C.G. Fichot, "Climate change leads to a doubling of turbidity in a rapidly expanding Tibetan lake", S*cience of The Total Environment*. 688 (2019) 952–959.

[4]   R. Garzon-Vidueira, R. Rial-Otero, M.L. Garcia-Nocelo, E. Rivas-Gonzalez, D. Moure-Gonzalez, D. Fompedriña-Roca, I. Vadillo-Santos, J. Simal-Gandara, "Identification of nitrates origin in Limia river basin and pollution-determinant factors", A*griculture, Ecosystems & Environment*. 290 (2020) 106775. https://doi.org/10.1016/j.agee.2019.106775

[5]   G. Goyenola, M. Meerhoff, F. Teixeira-de Mello, I. González-Bergonzoni, D. Graeber, C. Fosalba, N. Vidal, N. Mazzeo, N. Ovesen, E. Jeppesen, "Phosphorus dynamics in lowland streams as a response to climatic, hydrological and agricultural land use gradients", *Hydrol. Earth Syst. Sci. Discuss*. 12 (2015) 3349–3390. https:// doi:10.5194/hessd-12-3349-2015

[6]   P. Patel, A. Muteen, P. Mondal, "Treatment of greywater using waste biomass derived activated carbons and integrated sand column", *Science of The Total Environment*. 711 (2020) 134586. https://doi.org/10.1016/j.scitotenv.2019.134586

[7]   M. Majlesi, S.M. Mohseny, M. Sardar, S. Golmohammadi, A. Sheikhmohammadi, "Improvement of aqueous nitrate removal by using continuous electrocoagulation/electroflotation unit with vertical monopolar electrodes", S*ustainable Environment Research*. 26 (2016) 287–290.

[8]   O.A. Okunola, P.V. Santacroce, J.T. Davis, "Natural and synthetic receptors for nitrate anion", *Supramolecular Chemistry*. 20 (2008) 169–190. http://dx.doi.org/10.1080/10610270701747610

[9] J. Goel, K. Kadirvelu, V. Garg, A. Meena, R. Chopra, D. Chauhan, A. Rawat, S. Kumar, G. Mishra, C. Rajagopal, "A pilot scale evaluation for adsorptive removal of lead (II) using treated granular activated carbon", *Environmental Technology*. 26 (2005) 489–500.

[10] M. Talat, S. Mohan, V. Dixit, D.K. Singh, S.H. Hasan, O.N. Srivastava, "Effective removal of fluoride from water by coconut husk activated carbon in fixed bed column: Experimental and breakthrough curves analysis", *Groundwater for Sustainable Development*. 7 (2018) 48–55.

[11] M.J. Ahmed, S.K. Dhedan, "Equilibrium isotherms and kinetics modeling of methylene blue adsorption on agricultural wastes-based activated carbons", *Fluid Phase Equilibria*. 317 (2012) 9–14. https://doi:10.1016/j.fluid.2011.12.026

[12] B. Bestani, N. Benderdouche, B. Benstaali, M. Belhakem, A. Addou, "Methylene blue and iodine adsorption onto an activated desert plant", *Bioresource Technology*. 99 (2008) 8441–8444. https://doi: 10.1016/j.biortech.2008.02.053

[13] B.K. Nandi, A. Goswami, M.K. Purkait, "Adsorption characteristics of brilliant green dye on kaolin", J*ournal of Hazardous Materials*. 161 (2009) 387–395. https://doi.org/10.1016/j.jhazmat.2008.03.110.

[14] N. Wibowo, L. Setyadhi, D. Wibowo, J. Setiawan, S. Ismadji, "Adsorption of benzene and toluene from aqueous solutions onto activated carbon and its acid and heat treated forms: influence of surface chemistry on adsorption", J*ournal of Hazardous Materials*. 146 (2007) 237–242. https://doi.org/10.1016/j.jhazmat.2006.12.011.

[15] N.H. Mthombeni, L. Mpenyana-Monyatsi, M.S. Onyango, M.N. Momba, "Breakthrough analysis for water disinfection using silver nanoparticles coated resin beads in fixed-bed column", *Journal of Hazardous Materials*. 217 (2012) 133–140. https://doi:10.1016/j.jhazmat.2012.03.004

[16] M.S. Onyango, T.Y. Leswifi, A. Ochieng, D. Kuchar, F.O. Otieno, H. Matsuda, "Breakthrough analysis for water defluoridation using surface-tailored zeolite in a fixed bed column", *Industrial & Engineering Chemistry Research*. 48 (2009) 931–937.

[17] X. Han, E. Wishart, Y. Zheng, "A comparison of three methods to regenerate activated carbon saturated by diesel fuels", T*he Canadian Journal of Chemical Engineering*. 92 (2014) 884–891. https://DOI 10.1002/cjce.21910

[18] L. Lalitha, S.M. Mohan, "Performance evaluation of multibed adsorbent on removal of hexavalent chromium through various kinetic models", *Journal of Environmental Engineering and Landscape Management*. 26 (2018) 285–298.

[19] S.D. Faust, O.M. Aly, "Chemistry of water treatment", *CRC press*, 1998.

[20] P.H.K. Ouattara, B. Gouli, U. Kouakou, A. Dembele, A.T.A. Yapo, "Preparation and characterization of activated carbons based on peanut shell (Arachis hypogeae), green soya shell (Vigna radiate)", *International Journal of Science and Research* (IJSR). 3 (2014) 20014.

[21] T. Tiho, A.A. Adima, Y.C. Brou, N. Traoré, G.F. Kouassi, T.R. Kouamé, M. Kouba, "Borassus aethiopum Mart Ripe Fruits' Parts, and Drying Temperature Effect on Its Pulp Protein, Fat, Sugars, Metabolizable Energy and Fatty Acids Profile", *American Journal of Food and Nutrition*. 6 (2018) 67–75.

[22] M. Mazarji, B. Aminzadeh, M. Baghdadi, A. Bhatnagar, "Removal of nitrate from aqueous solution using modified granular activated carbon", J*ournal of Molecular Liquids*. 233 (2017) 139–148. https://doi.org/10.1016/j.molliq.2017.03.004.

[23] T.M. Albayati, K.R. Kalash, "Polycyclic aromatic hydrocarbons adsorption from wastewater using different types of prepared mesoporous materials MCM-41in batch and fixed bed column", *Process Safety and Environmental Protection*. 133 (2020) 124–136.

[24] S. Singha, U. Sarkar, "Analysis of the dynamics of a packed column using semi-empirical models: Case studies with the removal of hexavalent chromium from effluent wastewater", *Korean Journal of Chemical Engineering*. 32 (2015) 20–29. https://DOI: 10.1007/s11814-014-0183-3

[25] P. da L. Mesquita, C.R. Souza, N.T.G. Santos, S.D.F. Rocha, "Fixed-bed study for bone char adsorptive removal of refractory organics from electrodialysis concentrate produced by petroleum refinery", *Environmental Technology*. 39 (2018) 1544–1556.

[26] R. Bounif, "Conception d'une colonne à lit fixe au charbon actif granulé appliquée à l'étude dynamique de l'adsorption de bleu de méthylène", *Thèse de Doctorat'Université de BOUIRA* (2017) 193-194

[27] S. Marsteau, "Traitement des gaz dangereux captés sur les lieux de travail (institut national de recherche et de sécurité inrs)", *Département Ingénierie Des Procédés*. (2005).

[28] T.M. Darweesh, M.J. Ahmed, "Adsorption of ciprofloxacin and norfloxacin from aqueous solution onto granular activated carbon in fixed bed column", *Ecotoxicology and Environmental Safety*. 138 (2017) 139–145. http://dx.doi.org/10.1016/j.etap.2017.02.005

[29] J. López-Cervantes, D.I. Sánchez-Machado, R.G. Sánchez-Duarte, M.A. Correa-Murrieta, "Study of a fixed-bed column in the adsorption of an azo dye from an aqueous medium using a chitosan–glutaraldehyde biosorbent", *Adsorption Science & Technology*. 36 (2018) 215–232.

(2021) ; http://www.jmaterenvironsci.com